

XV-15 Tilt Rotor Research Aircraft Photogrammetry and Metrology Measurement

Haley Cummings
Mechanical Engineer
NASA Ames Research Center
Moffett Field, California, USA

Michelle Dominguez
Mechanical Engineer
NASA Ames Research Center
Moffett Field, California, USA

Eduardo Solis
Research Engineer
Science and Technology Corp.
Moffett Field, California, USA

Christopher Silva
Aerospace Engineer
NASA Ames Research Center
Moffett Field, California, USA

Belen Bowman
Aerospace Engineer
NASA Ames Research Center
Moffett Field, California, USA

Shirley Burek
Research Engineer
NASA Ames Research Center
Moffett Field, California, USA

ABSTRACT

A new measurement capability was created by combining photogrammetry and metrology techniques to accurately measure one half of the XV-15 Tilt Rotor Research Aircraft at the Smithsonian’s Udvar-Hazy museum. The challenges imposed by the fuselage and surrounding environment at Udvar-Hazy were overcome by careful application of photogrammetry and metrology techniques. Data analyses and processing included the use of multiple reverse engineering programs to accurately generate a complete 3-dimensional water-tight geometry of the aircraft and rotor blade. This paper describes the photogrammetry and metrology measurement systems, technology and hardware set-up, data analysis and processing methods, future work, and lessons learned. In addition, selected measurement results of the fuselage and rotor blade are presented.

INTRODUCTION

In 1973, NASA collaborated with the Army and began the development of the XV-15 Tilt Rotor Research Aircraft (TRRA) [1]. As a “technology demonstrator” program, two XV-15 were built and designated N702NA and N703NA. The aircraft were completed in 1977 by Bell Helicopter Textron Inc (BHTI). The aircraft were powered by twin Lycoming T-53 turboshaft engines and had two three-bladed 25-foot diameter rotors. The aircraft were designed with the ability

to fly in both helicopter mode and airplane mode, as well as maintain a 1-g level flight throughout the entire transition corridor during conversion. They had an estimated cruise speed of 300 knots at 12,700 feet altitude [2].

The XV-15 development program included 54 hours of wind-on wind tunnel testing of N702NA which culminated in September 1979, followed by an extensive flight test program beginning in April of 1979 with N703NA, as seen in Figure 1 [1,3]. Hence, substantial flight and wind tunnel data have been collected for this aircraft. N703NA is the only remaining XV-15 of the two built. It served from 1979 to 2003, successfully demonstrating operations under a variety of conditions and logging hundreds of hours of testing. This aircraft now resides at the Smithsonian’s Udvar-Hazy museum, as seen in Figure 2. There was previously, however, no consistent 3-Dimensional (3D) Computer Aided Design (CAD) model of the as-built vehicle. An accurate model of the vehicle was desired, since such a model can aid in simulation validation.

The NASA Revolutionary Vertical Lift Technology (RVLT) project performs research that supports the United States vertical lift industry and has previously performed research to compare simulations and wind tunnel test data of rotor blades [4,5], Unmanned Aerial Vehicles (UAVs) [6,7], and full-scale vehicles [8]. The Rotorcraft Aeromechanics Branch at NASA Ames Research Center (ARC) has previously demonstrated an ability to use photogrammetry and laser metrology systems to reverse engineer physical wind tunnel rotorcraft components and models.



Figure 1: XV-15 flight testing.

Presented at the Vertical Flight Society’s 76th Annual Forum & Technology Display, Virginia Beach, Virginia, USA, Oct. 6-8, 2020. This is a work of the U.S. Government and is not subject to copyright protection in the U.S.

As analytical and simulation-based engineering techniques have advanced at the same pace as computer processing power, the need for higher fidelity models has become critical to the advancement and validation of analytical and simulation tools. The accuracy and precision of predictive software is often limited by the accuracy and precision of the CAD model that is being utilized in the prediction. These considerations, coupled with the complete absence of CAD files for older models, a lack of as-designed CAD files for small UAV rotor blades, and a lack of other critical geometric data, have led to a need for reverse engineered as-built models obtained through optical techniques [9]. Measured models are typically used to create water-tight CAD geometries which reflect the as-built geometry and can be used in high-fidelity Computational Fluid Dynamics (CFD) simulation codes, which are then validated using wind tunnel data and flight data. The use of metrology for reverse engineering is quickly increasing in popularity and has been used by the Aeromechanics Branch at NASA ARC for several years.

Although long retired, the XV-15 remains relevant for rotorcraft research, in part because its design and test data are in the public domain. However, the XV-15 was designed and built in the 1970s, when digital documentation was in its infancy. This paper documents efforts to create a modern 3D CAD model from the actual aircraft.



Figure 2: XV-15 on display at the Smithsonian's Udvar-Hazy National Air and Space Museum.

Background

CAD models employed to generate mathematical grids for CFD have historically been lower fidelity CAD models due to the limitations of measurement systems. To use CAD models for CFD, the CAD must be water-tight as any blemishes in the surface will cause issues when generating CFD grids. As-designed CAD geometries do not account for the discrepancies that inevitably occur in the manufacturing process, and technical drawings likewise fail to account for the as-built geometries of parts.

Hand measurements using calipers, rulers, and micrometers are also found to be insufficient, especially when the object to be measured consists of free-form surfaces with complicated geometries found in vehicle fuselages and aerodynamic surfaces such as rotors and wings. Coordinate Measuring Machine (CMM) measurements offer high accuracy, though the poor resolution afforded by these machines results in coarse measurements. Likewise, photogrammetry offers high accuracy but poor target resolution when measuring thin and sharp geometries such as small-scale rotorcraft components and rotor trailing edges. However, photogrammetry has previously been successfully harnessed by the Aeromechanics Branch to accomplish measurements of wind tunnel models.

The rising accuracy and popularity of hand-held laser scanning devices has significantly enhanced the quality of as-built models that can be obtained. Hand-held scanners, like the MetraScan 70 in Figure 3 [10], are designed to capture complicated surface geometries, and often result in a point cloud that can be used to generate a water-tight CAD model. However, the method still requires careful application. Large geometries that require multiple scans to completely capture the geometry often incur data drift or misalignment during data processing. Thin, sharp geometries push the technology to its boundaries, as these types of edges are difficult to capture with any optical technique. Error can also be introduced during data processing, especially if there are significant gaps or noise in the data due to poor maintenance of the measurement systems.



Figure 3: MetraScan 70 handheld scanner [10].

To mitigate these introductions of error, laser scanning techniques were combined with photogrammetry techniques to accurately capture and post-process the XV-15. Photogrammetry techniques were previously utilized in the Aeromechanics Branch to obtain the outer mold line geometry of the quarter-scale V-22 wind tunnel model known as the Tilt Rotor Aeroacoustic Model (TRAM) [11]. To achieve this for the TRAM, targets were placed along the cross-section of the model at several locations on the fuselage. Using CAD software, a surface modeling tool was utilized to create a 3D model from the point cloud that was

obtained from the photogrammetry measurements. The process is depicted in Figure 4. Successful utilization of photogrammetry as a reverse engineering technique for the TRAM highlighted the possibilities of using photogrammetry as a complementary tool for laser scanning measurement techniques.

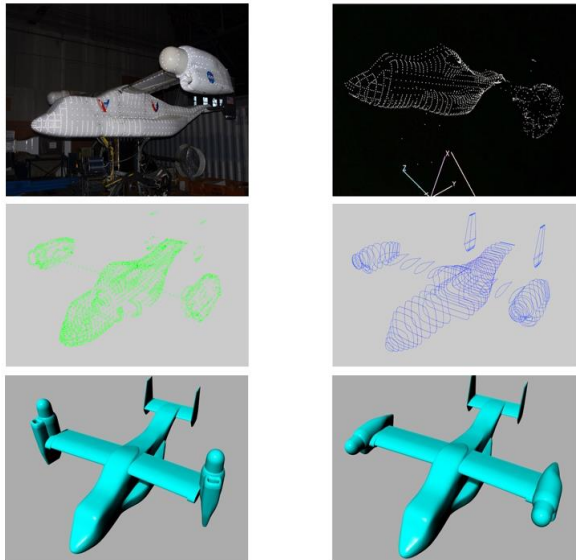


Figure 4: Tilt Rotor Aeroacoustic Model photogrammetry process. Top: setup and data acquisition. Middle: data processing. Bottom: 3D surface reconstruction in helicopter and airplane mode.

Photogrammetry techniques include the use of retro-reflective targets, a high-powered flash, and triangulation of the targets to establish the 3D location of the targets. Similarly, the laser scanning system uses retro-reflective targets to position itself in 3D space. Thus, the overlap of targets between the systems allowed for a high accuracy of photogrammetry to complement the high resolution of laser scanning.

In this paper two optical techniques are utilized: laser scanning and photogrammetry. Scanning hardware utilized included: Creaform’s C-TRACK dual camera sensor, MetraScan 70 handheld laser scanner, HandyScan 700 handheld laser scanner, and retro-reflective targets. To capture scan data, VXElements software was utilized. Photogrammetry hardware included: Geodetic Services Inc. V-STARS (Video-Simultaneous Triangulation and Resection System) Inca3a camera, custom made ¼” retro-reflective targets, coded targets, and scale bars. To capture photogrammetry data, V-STARS software was utilized. Post-processing software utilized to stitch and repair data, and to generate CAD models included Innovmetric’s PolyWorks software suite, specifically Inspector and Modeler, as well as Robert McNeel & Associates’ Rhinoceros 6 program.

The accuracy of the photogrammetry system is well-documented [12,13]. However, resolution of photogrammetry is limited to the size of the targets being measured. The resolution of the scanning system is easily set using VXElements software. The chosen resolution determines how much spacing occurs between each captured data point. However, while the manufacturer’s volumetric accuracy specification is 0.003 inches, it is unclear how much error is introduced due to data drift, data stitching, and data post-processing. This introduction of error is investigated herein, and further investigation is recommended.

METHODS

Udvar-Hazy Planning

To ensure that the proposed combination of photogrammetry and laser scanning techniques would be successful, modeling of the environment at Udvar-Hazy was completed prior to capturing the data. This was accomplished by modeling the room in which the XV-15 is located, roughly modeling the XV-15, and modeling the measurement systems. The requirements for a successful photogrammetry data capture were implemented into the simulation [14]. For example, each retro-reflective target must be photographed at least twice; a minimum of four to six images are required to self-calibrate the camera, and each image must contain at least twelve well-distributed retro-reflective targets and a minimum of four coded targets [14]. Thus, the placement of the retro-reflective targets and camera stations of each photograph were determined based on user experience and validating the camera stations in a simulated 3D environment as shown in Figure 5.

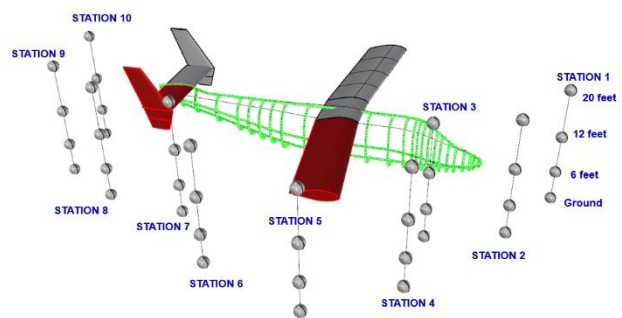


Figure 5: V-STARS camera stations were simulated prior to arrival at Udvar-Hazy.

Likewise, the volume in which a scan can take place is determined by the calibrated measurement volume of the laser scanning equipment. To ensure a minimum of at least 2 feet overlap for each scan section, the calibrated measurement volume was also simulated in a 3D environment. This also served to ensure accurate placement

of reference targets and alignment/stitching blocks. The 3D environment simulations allowed the scanning team to develop a robust measurement plan of action prior to setting foot at Udvar-Hazy. Once the team and equipment arrived to Udvar-Hazy, the plan was implemented, and a successful data capture was achieved.

Measurement Systems

Several measurement systems were utilized to perform the data capture of the XV-15 at Udvar-Hazy, including two laser scanning systems and one photogrammetry system. In addition, an inclinometer was used, and digital photographs of the work performed documented the entire process.

Photogrammetry

The digital image-based photogrammetric hardware and software system, V-STARS, was developed by Geodetic Systems, Inc. Figure 6 shows the V-STARS optical hardware installed on the XV-15. This V-STARS system measures 3D coordinates of retro-reflective targets (points of interest) by intersecting lines of sight from the cameras to the points using triangulation [15–17]. The 3D measurement uncertainty of current V-STARS systems ranges from $10 \mu\text{m} + 10 \mu\text{m}/\text{m}$ to $5 \mu\text{m} + 5 \mu\text{m}/\text{m}$, the latter uncertainty corresponding to $0.001'' @ 160''$ or 1:160,000 [12,13]. V-STARS has been used previously for calibrations and measurements at ARC, including calibration of the TTR [18] and to measure the geometry of the Tilt Rotor Aeroacoustic Model (TRAM) [11].



Figure 6: Photogrammetry targets installed on the N703NA XV-15 at Udvar-Hazy.

Laser Scanning

The two non-contact (3D) optical laser scanning measurement systems are designed by Creafom and utilize

Creafom’s in-house scanning software, VXElements. This hardware can be seen in Figures 3 and 7 [10,19]. VXElements has a Graphical User Interface (GUI) that allows the user to observe what they are scanning and allows them to observe where data has not yet been captured in real time. The GUI also allows the user to calibrate the hardware using factory calibration equipment. The user specifies the measurement volume in which they will scan depending on the size of the object, and the calibration is performed for the specified measurement volume using a calibrated scale bar, targeted plate, or targeted sphere.

The MetraScan 70 is a professional optical CMM scanning system composed of a workstation laptop, C-TRACK dual-camera sensor, and an arm-free handheld laser with external referencing targets. The system measures objects within the calibrated volume set by the C-TRACK. The C-TRACK has specialized optics and lighting to triangulate the position of the handheld laser with built-in reflectors. Surface acquisition is done by observing the laser lines projected onto the surface and data is registered depending on the triangulated position. The system is capable of dynamic referencing by placing optical reflectors on the object, dynamically extending the measurement volume without the loss of accuracy and with immunity to vibrations and thermal variations in unstable environments [20].

The HandyScan 700 is a stand-alone device composed of a workstation laptop and a small portable handheld laser scanner and requires no external tracking system. The system uses triangulation and binocular vision (two camera sensors) to self-position itself to a unique dynamic



Figure 7: Creafom's HandyScan 700 handheld laser scanner (left) and C-TRACK dual-camera sensor (right) [10, 19].

referencing system with the use of positional targets which are fixed onto the surface of an object to ensure repeatability, self-tracking, and accuracy.

Both of these optical laser systems from Creaform have undergone testing by Creaform and have been previously used as measurement tools both at ARC (as mentioned previously in references [4,5,7,21]) and in industry [20–25].

Measurement Systems Setup

The photogrammetry and laser scanning systems require careful and methodical preparation and setup prior to use. The V-STARS retro-reflective targets must be placed carefully and with precision. V-STARS post-processing software allows for the averaging of the location of points, but still relies on the overall accuracy of the placement of positional targets to capture specific locations marked by those targets. Likewise, the placement of positioning targets for the laser scanning systems is not so critical for accuracy of the scan, but the installed location of the targets determines the scan volume that can be captured in each scan, and also determines how easy it is for the user to complete the scan. For this work, the museum attendants at Udvar-Hazy required that any targets placed on the vehicle be removed with no residue left behind. The material of the retro-reflective targets is difficult to remove from surfaces, so painter's tape was used in between the retro-reflective material and the outer skin of the fuselage. The adhesive method allowed for easy and quick clean up, as each individual target did not have to be removed. Instead, the strip of painter's tape containing all of the targets was removed with no damage to the aircraft's paint.

Photogrammetry

As mentioned previously, the placement of the hundreds of V-STARS retroreflective targets was planned out prior to the arrival of the team to Udvar-Hazy. Each target served a specific purpose. For the V-STARS triangulation and resection algorithms to function, a minimum number of targets (twelve) must be included in each image, and each target that is captured must be photographed a minimum of two times throughout the photo shoot.

Custom-made retroreflective targets were placed at several cross-section locations on the XV-15 from the nose to the tail. First, a strip of painter's tape was placed around the starboard side of the fuselage. Then, ¼" diameter retro-reflective targets were placed, equally spaced, on the masking tape. The cross-section locations were determined based on the technical drawings of the vehicle that showed cross-section views of the fuselage from the nose to the tail.

Using the same application method, targets were also placed tracing the outer mold lines of the starboard side of the fuselage. Specifically, targets were placed along the curves that outlined the sponsons and the transition from the fuselage to the wing. Targets were placed on the port side of the fuselage and wings as well. This was done to ensure minimal data drift when the starboard data was post-processed and mirrored to create the port side data. The targets captured on the port side acted as indication that the mirroring was achieved successfully, and that the mirrored data was tangent to the original data.

To obtain accurate data using photogrammetry, extra targets are required as "fill-in" targets. These targets serve no other purpose than to fill-in otherwise target-scarce locations (where no data is otherwise captured) on the fuselage and to provide the necessary extra targets. So-called "coded targets" are also required for successful utilization of the V-STARS photogrammetry system. These thin, square, plastic objects have a specific identifiable pattern of targets on them that the V-STARS software recognizes and uses to triangulate and stitch together all other targets from the photographs. Scale bars are long carbon fiber bars with coded targets affixed to them that give the photo shoot scale and allow the software system to dimension the target locations in 3D space. There are two required scale bars for a V-STARS photogrammetry shoot, and they must be placed perpendicular to each other.

Camera stations, or the locations at which photos were to be taken from, were predetermined during the planning stages of this work, as seen in Figure 5. A scissor lift was required to acquire images from all angles around the vehicle. The scissor lift allowed photos to be taken from above the fuselage along the entire starboard side of the fuselage, as well as from above and behind the tail. Figure 6 shows the XV-15 with photogrammetry targets installed.

Laser Scanning

Using the adhesive method as described above, the positioning targets for the Creaform system were affixed to the fuselage. The C-TRACK requires that a minimum of four reference targets are seen at all times by the C-TRACK cameras. Adding additional targets improves the accuracy of the system when measuring large-scale objects. The placement of reference targets is critical to prevent the user from blocking the targets while scanning and to ensure measurement volume overlap of reference targets for stitching. The reference targets were carefully planned out for the XV-15. Extra reference targets were used as fill-in targets to ensure dynamic referencing continued in tight, complex areas and to ensure visibility of at least four reference targets was maintained at all times to avoid freezing of the system. When the system freezes, there is the

potential for data drift due to the loss of dynamic referencing while scanning.

The aircraft was scanned in multiple sections to capture the entire fuselage, and custom alignment blocks were required at the areas of overlap so that data stitching and alignment could be accomplished. Ideal overlapping geometry is 3D in nature so that the software has multiple dimensions to reference when stitching. Thus, two-inch cubes were painted white and affixed to the fuselage using 3M adhesive squares. The cubes with 3M adhesive were affixed to masking tape which was then placed on the fuselage. Reference targets were also placed on the cubes. The cubes were used to help stitch the scans and align the data between the two measurements systems. In addition, though the Creaform system cannot recognize V-STARS retro-reflective targets, the V-STARS system was able to measure all of the Creaform positioning targets and utilize their location in 3D space to create an origin for the measurements and compare the measured points between V-STARS and Creaform.

As a majority of the fuselage is white, the laser scanning system easily measured the surface. However, the glass windows of the cockpit posed a problem to laser scanners. To mitigate this issue, the glass windows of the cockpit were covered with butcher paper and secured using masking tape. The paper was not installed completely flat, so there were ripples in the data. This was accounted for in post-processing.

Because the MetraScan must be in visual contact at all times with the C-TRACK, it is difficult to scan low visibility areas such as the wheel well cavities and other recessed areas. In addition, the MetraScan has a relatively bulky size that cannot fit into areas such as the spinner intake cavities and wheel wells. The comparatively slender size of the HandyScan, however, makes it ideal for the cavities, and it was used to collect data in hard to reach areas with low visibility and low volume surface areas of the aircraft. The HandyScan requires at least four positioning targets are in view at all times. These targets are used by the scanner to position itself in the calibrated volume relative to features and targets it has already scanned. It is crucial that the targets stay stationary relative to one another during the duration of the scan. The HandyScan system consists of the portable handheld scanner, workstation laptop, power cable, USB cable that connects the scanner to the laptop, and reference/positioning targets.

DATA ACQUISITION

Photogrammetry

Once the V-STARS retro-reflective targets were installed on the model, the scale bars were arranged perpendicular to

each other, and the scissor lift was brought into position, the V-STARS images were captured. This set up process took approximately 1.5 days and the data capturing process took approximately 45 minutes. During the data capture, the scissor lift was moved several times so that the entire XV-15 could be captured from several angles. Approximately 600 images were taken, and 2300 targets were captured. Immediately following the data capture, an initial post-processing sequence was performed to ensure the data quality was satisfactory. Figure 8 shows the raw photogrammetry data displayed in the V-STARS software.

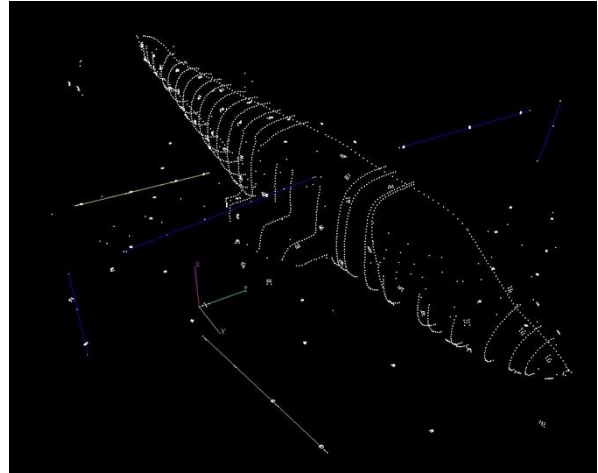


Figure 8: V-STARS data captured and displayed in V-STARS software.

Laser Scanning

The MetraScan 70 and C-TRACK system can only scan within a 12 cubic meter calibrated volume. Thus, the set-up procedure for this system was repeated several times to capture the entire XV-15 fuselage. Within each set up location on the main fuselage, the MetraScan was set to scan at a resolution of 2 mm. This relatively coarse resolution was deemed satisfactory because the free-form fuselage surface does not (within 2 mm) rapidly change geometry. For locations such as the rotor, 0.2 mm resolution was used to adequately capture the complicated geometry. Figure 9 shows team members scanning the XV-15. Each time the



Figure 9: Scanning the XV-15.

user wishes to review the data, they must pause the scan. Pausing the scan forces the VXElements software to update the graphics model which appears inside the GUI. With high resolution or high data content scans, this pausing and updating can take several minutes, though it is required in order to save the scan. Once the scan has been paused, the current point cloud model can be viewed and inspected to ensure measurements are within system accuracy. This allows the user to identify gaps in the data where additional scanning is necessary. This is especially useful for large scans, as it is easy to forget which data has previously been scanned.

Scanning of the aircraft took 2 days. To scan an entire half of the XV-15, it was necessary to lay down under the aircraft, use a scissor lift to reach the top of the aircraft, and scan at every point in between the extremes. As such, the entire team at Udvar-Hazy participated in scanning the fuselage. To scan efficiently, the user must hold the MetraScan 70 at an optimum distance (calibrated range) from the object to be scanned. This is indicated to the user by a color bar which shows red if the scanner is held exceptionally close to the object, yellow if the scanner is held slightly too close to the object, green when the scanner is at the optimum distance away from the object, light blue when the scanner is slightly too far, and dark blue when the scanner is exceptionally far from the object, as seen in Figure 10. The scanner also performs optimally when the object being scanned is perpendicular to the scanner. For smooth, free-form large-scale geometries, this can be difficult to achieve. It is also physically taxing for the user when holding the scanner far away from their body. The scanner still collects data if the scanner is not held at the optimal distance or angle relative to the scanned object, but the data collection rate is reduced.



Figure 10: VXElements GUI helps the user maintain optimal laser distance from the object surface.

Scanning with the HandyScan 700 closely mirrored that of the MetraScan, although the HandyScan is connected to the computer workstation via a cable. The HandyScan 700 uses the same VXElements software as the MetraScan 70. This scanner was used in hard to reach locations such as the wheel wells and inside the sponsons intake cavities, which were impossible to capture with the MetraScan 70 due to blockage.

As the MetraScan 70 was maneuvered strategically so that all of the XV-15 fuselage could be measured, the C-TRACK was as well. The C-TRACK and MetraScan 70 must maintain constant visual contact, as mentioned before, so the C-TRACK positioning was as critical as the ability to move the MetraScan around the vehicle. Methods to maintain visual contact between the two systems included rolling the C-TRACK 90 degrees so that the two cameras were at different vertical locations rather than at different horizontal locations, lowering the C-TRACK so that it was almost resting on the floor, and elevating the height of the C-TRACK on man lifts or scaffolding. In addition, due to the complexity of the aircraft, extra fill-in reference targets were added to ensure the C-TRACK and VXElements did not freeze while performing data capture. When the software and C-TRACK freeze due to the loss of reference targets, dynamic referencing is lost. While the C-TRACK can regain dynamic referencing when reference targets are visible again, there is a higher probability of the data shifting or warping during loss of dynamic referencing.

DATA PROCESSING

Prior to processing the point cloud data, paper technical drawings of the aircraft were provided by the U.S. Army Technology Development Directorate via PDF scans which were then converted to digital 3D CAD drawings. The digital drawings were used as the as-designed baseline model for comparison and to assist with data orientation, nacelle translation and overall alignment to document similarities and differences between the as-designed drawings and as measured data. A highly accurate 3D model of the aircraft using the technical drawings has yet to be constructed due to the limited amount of information between areas of complex transition and intersection such as the wing and fuselage, tail and fuselage, and the nacelle and wing.

While at Udvar-Hazy, at the end of each day, the scans were quickly stitched, as seen in Figure 11, to ensure the laser and C-TRACK were performing within manufacturer specifications. The laser system was calibrated at the start of each day to ensure accurate measurements were always acquired. The largest point cloud file of the 13 scanned

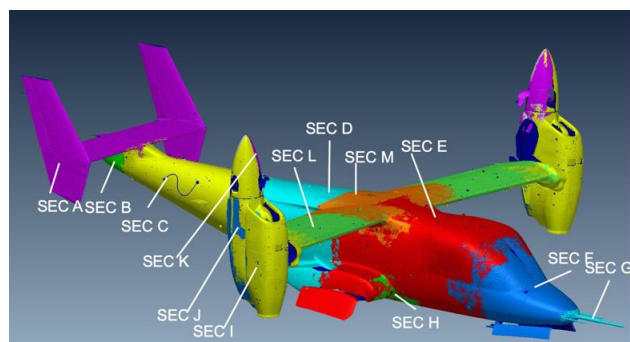


Figure 11: 13 stitched scan sections of the XV-15.

sections used over 3 gigabytes of memory. Once all of the XV-15 scanning and photogrammetry data was captured at Udvar-Hazy, point cloud post-processing software was utilized to repair the data, mirror the data, and create NURBS (non-uniform rational basis spline) surfaces. These NURBS surfaces were validated against the original scan data and photogrammetry data to ensure minimal errors were introduced during post-processing. Finally, an as-built water-tight model was obtained.

PolyWorks

The point cloud editing software used for this work was Innovmetric’s PolyWorks. PolyWorks has two modules: Inspector and Modeler. The Inspector module is used to edit the raw point cloud file and manually remove noise. The module also allows for the alignment of multiple scans into one file. The origin is manually set in the Inspector module, and finally the point cloud file is converted into a polygonal mesh. Modeler is used to repair the data, fill and reconstruct any data gaps, and smooth the data. Once the data are clean, curves are manually fitted to the point cloud. Finally, the generated curves are used to section the model into NURBS surfaces, as seen in Figure 12. These NURBS patches cover the entire model and allow the user to generate a water-tight model. This water-tight model can be used for simulations including CFD, as well as for 3D printing among other applications.

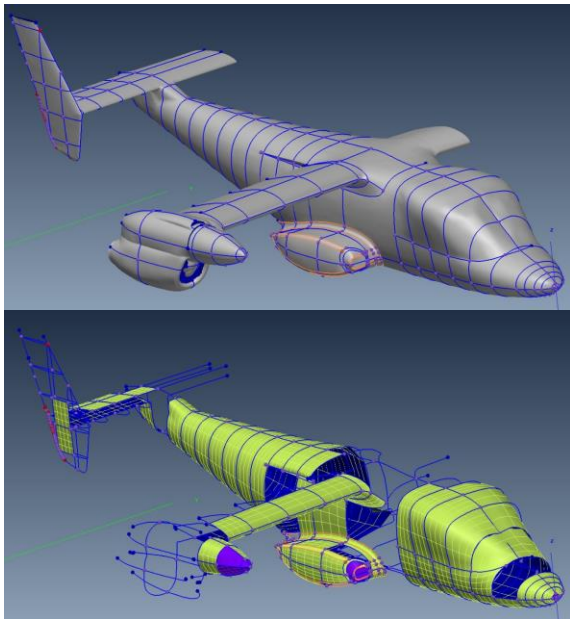


Figure 12: Mold line curves (top) are used in PolyWorks to create four-sided NURBS surfaces (bottom).

PolyWorks Modeler is optimized to edit polygonal meshes, so the polygonal mesh created in Inspector is imported into the Modeler module. There are various tools within the module which can be utilized to fill data gaps and repair

corrupted data. The data can also be smoothed in Modeler. Once the holes in the data have been filled and the data have been otherwise repaired, cleaned, and smoothed (see Figure 13), outer mold lines and cross-section curves of the model are generated. These curves enable the creation of NURBS surfaces. The NURBS model was exported from Modeler and imported into Rhinoceros 6 (Rhino) for further editing.

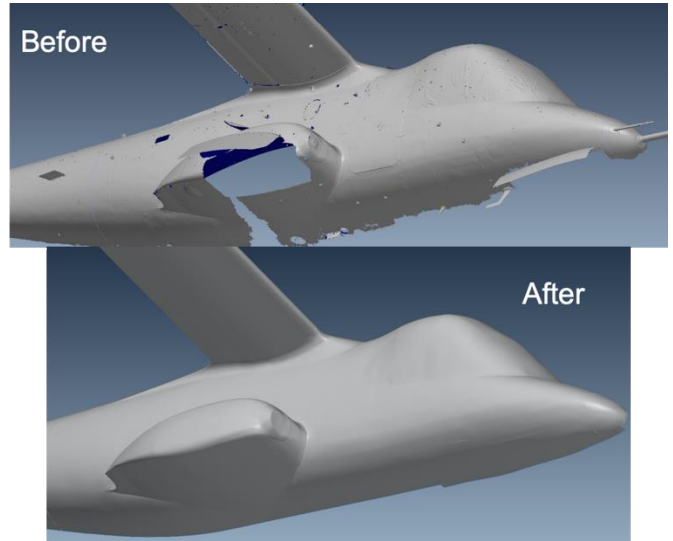


Figure 13: Repairing and smoothing the XV-15 point cloud in PolyWorks.

Rhinoceros 6

Exporting the NURBS models from PolyWorks Modeler resulted in problematic geometry that required further repair. This included the presence of non-manifold edges, which are defined as any edge that is shared by more than two faces. Another topological anomaly encountered was the direction of the mesh UVW normal vectors. The “U” and “V” vectors represent the horizontal and vertical directions, respectively, of a 2D plane assigned to a 3D surface. The “W” direction is perpendicular to “U” and “V” directions. Proper modeling techniques require that all normal vectors (“W” direction) should agree in their direction. These repairs can be seen in Figure 14.

Rhino was also used to repair locations on the model where insufficient data was captured. Rhino modeling methods are more efficient for completing these repairs. Namely, the full nacelle was impossible to scan, so Rhino in conjunction with technical drawings was used to repair the geometry, as seen in Figure 15.

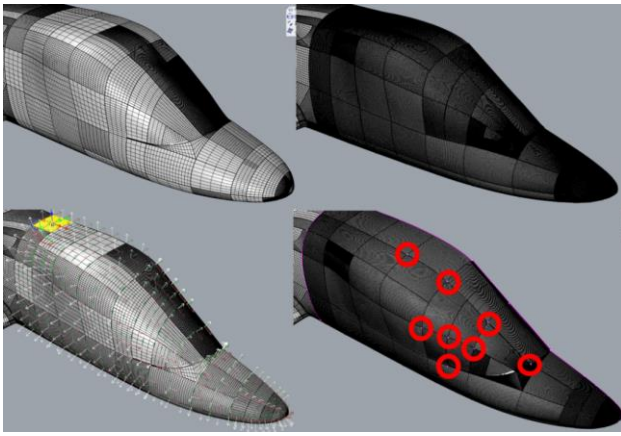


Figure 14: Repair of surfaces in Rhino. Top: smoothing of surfaces. Bottom left: correcting UVW normals. Bottom right: Correcting manifold edges.

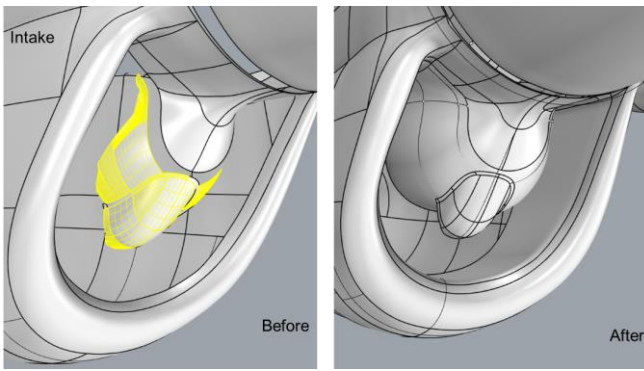


Figure 15: Nacelle repair in Rhino. The intake of the nacelle was inaccessible by scanner, so it was manually repaired by referencing technical drawings.

The final geometry was required to be water-tight for grid generation CFD purposes, so the model was verified for this condition and further repairs were made to ensure that it was water-tight. Thus, the result of the data processing is an as-built 3D CAD model of the N703NA XV-15 in helicopter mode and in airplane mode, as seen in Figure 16. This CAD model is available in STEP, IGES, or STL format and is ready for use to generate grids for CFD codes.

DATA ANALYSIS

Several methods were utilized to ensure that data quality and accuracy were maintained throughout the post-processing procedures. Fundamentally, the V-STARS photogrammetry data was used to validate scan stitching

and data mirroring using both Rhino and PolyWorks. The PolyWorks Inspector module has functions built in which allow for the convenient comparison between various models. Thus, after each repair step, the repaired model was compared to the original scan data.

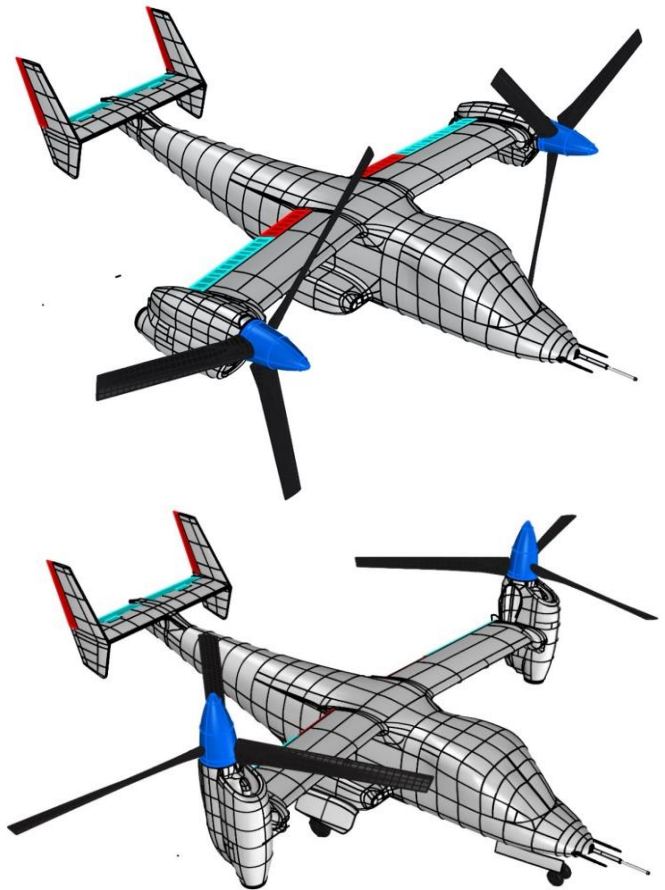


Figure 16: Final water-tight CAD model in airplane mode (top) and helicopter mode (bottom).

As mentioned previously, the scan was completed in sections, and each section contained several reference targets which provided overlap between scanning sections.

Both the scanning software and the photogrammetry software were able to store the location of these reference targets. Thus, these targets were used to accurately stitch the scan sections together using post-processing software as seen in Figure 17. V-STARS tool suite can yield an accuracy of

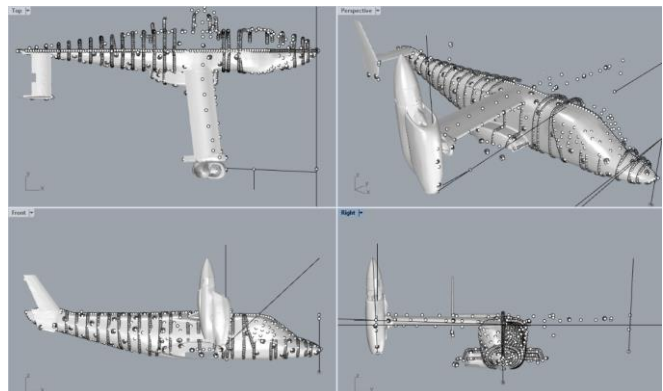


Figure 17: V-STARS data and scan data imported into Rhino for accurate stitching of scans.

.0005 inches for target measurement. The volumetric accuracy of the Creaform scanners is 0.003 inches. By utilizing these systems in tandem and utilizing V-STARS to ensure accurate stitching of the scans, the overall accuracy of the scan was maintained.

After the data was stitched together, the reference targets in the stitched sections as located by the scanning system were compared against the same reference targets that were captured by the photogrammetry system. This was done because though the scanning system captured the data in sections, the photogrammetry system captured all of the data at once. Thus, by comparing the two, the accuracy of the stitching of the scanned sections could be attained. Figure 18 illustrates the location of the different sections that were analyzed. The reference targets as captured by the scanning system and the photogrammetry system were overlaid and compared. The difference between the X, Y, and Z coordinate locations of each reference target was computed. Table 1 shows the average difference between coordinate locations for the reference targets in each section and shows the average overall difference for all 7 sections that were compared here. From this data, it is clear that no data drift was introduced by the C-TRACK camera or reference targets, and that negligible error was introduced in the stitching of sections.

Table 1: Comparison between coordinate locations of reference targets extracted from scanning system and photogrammetry system.

	Average (inches)		
	ΔX	ΔY	ΔZ
Section 1	-2.22E-16	-3.33E-05	-3.33E-05
Section 4	-3.33E-05	3.33E-05	-4.74E-15
Section 6	0	2.37E-15	-7.11E-15
Section C1	-1.85E-02	2.20E-02	9.57E-03
Section D	0	-2.37E-15	-4.74E-15
Section E	0	3.33E-05	6.67E-05
Section F	0	9.47E-15	-4.74E-15
Total Avg.	-2.65E-03	3.14E-03	1.37E-03

A single NURBS patch created in PolyWorks is generated based on four-sided closed/intersecting curves fitted to random points (within laser resolution) instead of neighboring surface patches. This method of fitting curves to random points does not allow for uniform surface modeling in PolyWorks. Therefore, the grid is not uniform and the UVW vectors are correctly outward, but randomly generated in PolyWorks. To overcome the random modeling in PolyWorks, Rhino was used to reorient all the UVW normals and all surface patches were re-gridded for uniform point density between sections. In some cases, due to split edges from the NURBS surfaces from PolyWorks, re-gridding did

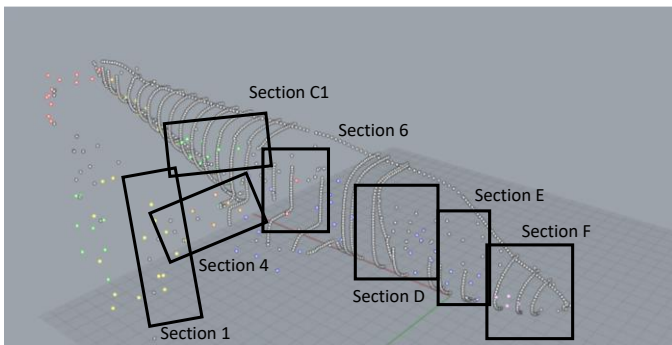


Figure 18: Reference targets from the scanning system and the photogrammetry system overlaid. The coordinate locations of these points were compared.

Once the repaired model was ready to be exported out of PolyWorks Modeler and into Rhino, the data were first compared against the raw point cloud data to ensure that minimal error was introduced in the PolyWorks repair post-processing errors. As seen in Figure 19, the repaired model stayed within 0.04 inches of the original scan point cloud.

Similarly, with each repair step that was performed in Rhino, the repaired data were compared to the raw point cloud data. These analysis steps ensured that the final discrepancies between the raw scan data and the post-processed, repaired model were minimized and quantified through each step.

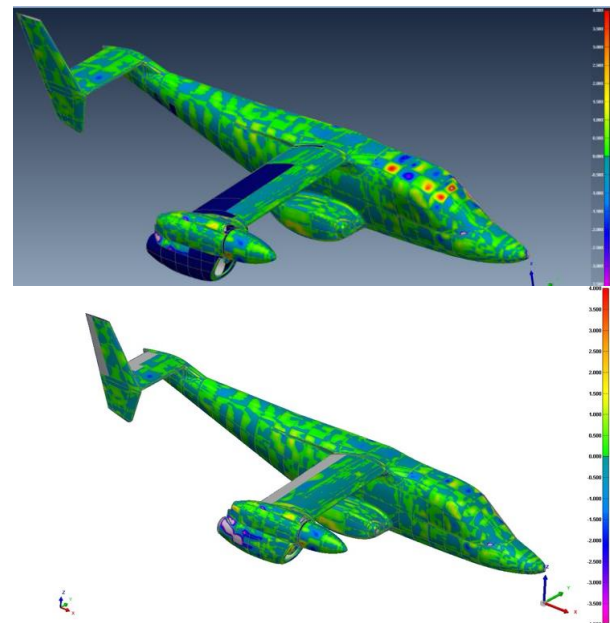


Figure 19: Fit check between raw point cloud data and Rhino CAD (error bar on right in mm). Top shows first iteration and bottom shows improvement in correlation with further iterations.

not always work, and the surface patches were rebuilt using the curves from PolyWorks and extracted iso-curves. The endpoints of the curves were corrected because the problematic curves had dual points, which affects all other neighboring surface patches causing non-manifold edges. For each non-manifold edge, four surrounding patches had to be manually rebuilt.

The re-gridding for each patch was set to 50 UV points to ensure error was not introduced into the as-measured geometry. This method was used for all correctly exported patches because Rhino can calculate the deviation error when re-gridding a surface patch. Manually rebuilt surface patches in Rhino do not calculate a surface deviation error, and it is an extensive manual process to ensure the patches are accurately rebuilt.

50 UV points provided an average error of about 0.0003 in which is insignificant error. The surface deviation between the Rhino updated geometry, the raw point cloud, and processed points clouds were used to ensure the new data was representative of the as-is measurements. In addition, the corrected patches make the process easier to convert many patches into single large surface patches to prepare the geometry for CFD as shown in Figure 20.

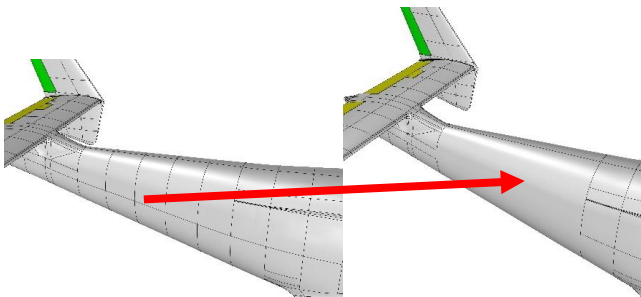


Figure 20: Surface simplification in Rhino. Left shows before simplification and right shows after simplification.

Rotor Blade Comparison

For 2D blade to blade comparison between as-designed blades (based on engineering drawings), wind tunnel blades (blade tested at ARC and currently stored at ARC) and experimental flight blades (flight testing conducted with this blade, currently installed on N703NA at Udvar-Hazy), the cross-sections at $r/R = 1.0$ were extracted and plotted over each other. Differences at the blade leading and trailing edges can be seen between as-designed, wind tunnel, and experimental rotor blades as shown in Figure 21. Based on reviewing the technical drawings, the as-designed rotor blade does not account for dimensional changes that are added during the manufacturing process. In this case, paint thickness was not accounted for in the as-designed process.

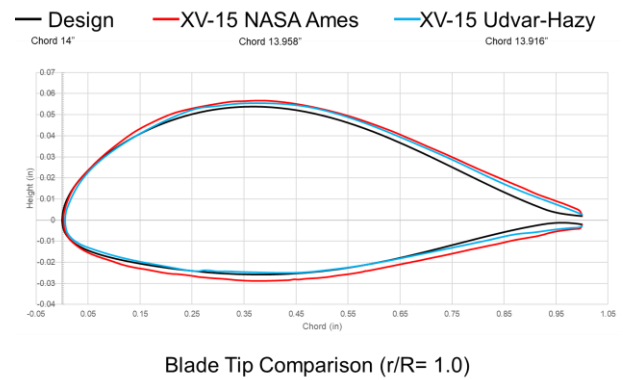


Figure 21: Blade tip comparison at $r/R = 1.0$ of as-designed rotor blade vs NASA Ames wind tunnel rotor blade vs Udvar-Hazy experimental rotor blade.

The ARC wind tunnel blade experienced paint erosion at the leading edge, but not as significant as the experimental flight rotor blade at Udvar-Hazy, which can be seen in Figure 22. The paint eroded off the rotor blade leading edge, exposing the bare metal rotor blade. In addition, blade thickness from the mid-chord to trailing edge can be seen in both wind tunnel and flight blades. The wind tunnel rotor blade shows a thicker transition due to three layers of paint versus two layers of paint for the experimental flight rotor blade. The difference in chord thickness can affect the results for calculating coefficients of lift and drag due to the rotor blades experiencing the largest centrifugal force at the rotor tip.



Figure 22: Paint erosion at the leading edge of the experimental flight blade at Udvar-Hazy.

The aforementioned is only a 2D comparison between the three rotor blades. The as-designed rotor blade needs to be modeled in 3D and the wind tunnel rotor blade scan needs to be processed for 3D blade-to-blade comparison. The experimental flight blade was post-processed and repaired using PolyWorks software. The repaired blade showed good agreement with the original point cloud, as the deviation was, for the majority of the blade, within 0.001 inches as seen in Figure 23.

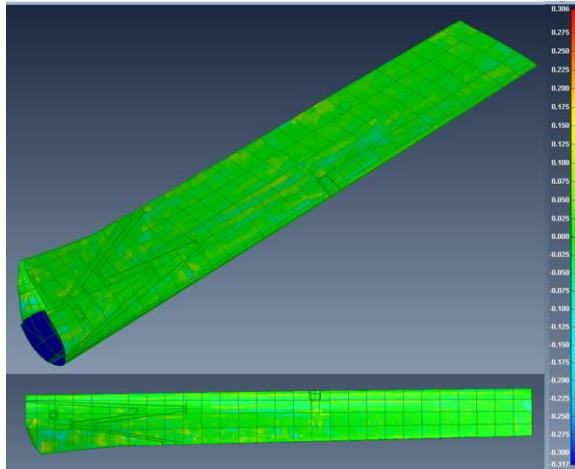


Figure 23: Post-processed rotor blade in comparison to raw point cloud. Error bar on right in mm.

FUTURE WORK AND LESSONS LEARNED

Future Work

To further validate the accuracy of the reverse engineering process described herein, the aligned data should be opened in PolyWorks Modeler software. In the overlapping data regions, cross-sections can be projected and the delta between the cross-sections can be measured.

This data extraction and comparison will increase user confidence in the accuracy of the scanning system and will show the accuracy achieved in combining laser scanning and photogrammetry to complete a reverse engineering project of this scale.

This data extraction and comparison will increase user confidence in the accuracy of the scanning system and will show the accuracy achieved in combining laser scanning and photogrammetry to complete a reverse engineering project of this scale.

Lessons Learned

Though the XV-15 aircraft fuselage was successfully measured and post-processed into a water-tight CAD model, many lessons were learned throughout the process that will make future vehicle measurements more efficient and streamlined.

In future measurement sessions, photogrammetry should be used to measure the entire XV-15 instead of just half of the aircraft. The number of cross-sections could be reduced, though the number of targets should be increased. In addition, to increase the ability to rapidly and efficiently

stitch multiple scans together using the V-STARS targets, custom target plates should be designed and implemented.

To reduce the size of the scan data file and to reduce the scanning time, the scan resolution can be made coarser for simple surfaces. The resolution for this project was set to 2 mm for the simple surfaces of the XV-15. For simple surfaces, the number of points in the point cloud needed to describe the simple geometry is much less than for complicated surfaces. The recommended resolution for the main body is no finer than 5 mm. In addition, prior to the start of scanning the aircraft, all reference targets should be scanned first with the C-TRACK in sections. This ensures the reference targets do not experience creep due to thermal expansion or poor manual installation and will help to avoid introducing error into the data.

With the original planning for this project, the scanning of the main fuselage was considered most important. However, in the post-processing, the details of the wing and tail trailing edges were much more difficult to repair, and critical design features such as gurney flaps and access panels were encountered that were not included in the as-designed technical drawings, which increased the total scanning time. The inboard section of the nacelle was also not scanned well at Udvar-Hazy due physical limitations from the wing and nacelle orientation. This section was also not easy to repair during post-processing. In future data collection sessions, it is recommended that coarse scanning resolution be used to reduce scanning time for simple geometry and more time be spent using fine resolution to capture complicated geometry.

Finally, though the XV-15 was roughly symmetric, a more accurate model could have been generated if both sides of the aircraft had been captured. This would have taken significantly more time, however, so for future projects, the cost/benefit analysis needs to be considered regarding whether the slight gain in accuracy is worth the additional scanning and post-processing time. It is the belief of the authors that this additional time is well-worth it to obtain more accurate measurements.

CONCLUSIONS

A new metrology capability was coupled with digital photogrammetry to accurately measure the XV-15. The challenges imposed by the XV-15 surface typology and the surrounding environment at Udvar-Hazy were overcome by careful application of photogrammetry and metrology techniques. In addition, a single rotor blade was measured on the XV-15. Accomplishments and findings are below:

1. Metrology technique was used to enhanced NASA's capability to accurately measure full-scale aircrafts.
2. Photogrammetry technique and 3D CAD software

were used to align and orient the point cloud sections into a single point cloud.

3. Highly accurate water-tight as-is 3D CAD geometries of the XV-15 and rotor blade were generated in two configurations: airplane and helicopter mode. These models are useful for grid generation for use in CFD simulation codes.
4. A 2D blade-to-blade comparison between as-designed, wind tunnel, and experimental flight rotor blades was performed.

ACKNOWLEDGMENTS

The authors would like to thank NASA's RVLТ project and the United States Army Technology Development Directorate for their contributions to the funding of this work. Gratitude is also extended to the Udvar-Hazy employees for their assistance during the data acquisition. Kristen Kallstrom is thanked for her help in processing IT paperwork. Witold Koning and Ethan Romander are much appreciated for building the PolyWorks workstation. Wally Acree's insightful comments and immense knowledge that he provided is valued greatly. The 2017 Fall Aeromechanics Branch Interns are also thanked for their help with scanning preparations.

REFERENCES

- [1] Maisel, M. D., Giulianetti, D. J., and Dugan, D. C., 2000, *The History of the XV-15 Tilt Rotor Research Aircraft: From Concept to Flight*, National Aeronautics and Space Administration, Washington, D.C.
- [2] Maisel, M. D., 1975, *NASA/Army XV-15 Tilt Rotor Research Aircraft Familiarization Document*, NASA/TM-X-62, 407, Moffett Field, California.
- [3] Sammons, L., 1985, "XV-15 (NASA 703) Evaluation Flight at Ames Research Center" [Online]. Available: https://ails.arc.nasa.gov/images/ARCHIVE/Imaging CD/Imaging CD %23696/AC85-0186 folder/AC85-0186 jpg/highres/54927_AC85-0186-8.jpg. [Accessed: 22-Jun-2020].
- [4] Perez Perez, B. N., 2018, *Rotor CFD Analysis at Terrestrial and Martian Atmospheric Densities*, NASA/CR-2018-219780, Moffett Field, California.
- [5] Koning, W. J. F., 2018, *Generation of Performance Model for the Aeolian Wind Tunnel (AWT) Rotor at Reduced Pressure*, NASA/CR-2018-219737, Moffett Field, California.
- [6] Ventura Diaz, P., and Yoon, S., 2018, "High-Fidelity Computational Aerodynamics of Multi-Rotor Unmanned Aerial Vehicles," *AIAA Aerospace Sciences Meeting, 2018*, American Institute of Aeronautics and Astronautics Inc, AIAA, Kissimmee, Florida.
- [7] Koning, W. J. F., Russell, C., and Theodore, C., 2018, *Mid-Fidelity Computational Fluid Dynamics Analysis of the Elytron 4S UAV Concept*, NASA/TM-2018-219788, Moffett Field, California.
- [8] Kottapalli, S., Acree, C. W., and Jr., 2019, "Correlation of Full-Scale Isolated Proprotor Performance and Loads," *75th Annual Forum and Technology Display*, AHS International, Philadelphia, Pennsylvania.
- [9] *Reverse Engineering with 3D Measurement*, [White Paper], Faro, Inc., Retrieved from https://www.faro.com/wp-content/uploads/download-center/download-centre/whitepaper_reverse-engineering-with-3d-measurement.pdf?sfvrsn=4.
- [10] Creaform, *Optical CMM Scanners: MetraSCAN 3D*, Retrieved from: https://www.creaform3d.com/sites/default/files/assets/brochures/files/metrascan/2014/metrascan3d_brochure_en_hq_25062014.pdf.
- [11] Young, L. A., 1998, "Tilt Rotor Aeroacoustic Model (TRAM): A New Rotorcraft Research Facility," *AHS International Meeting on Advanced Rotorcraft Technology and Disaster Relief*, AHS International, Gifu, Japan.
- [12] Sandwith, S., and Cork, G., 2000, "V-STARs/M System Accuracy Test Results," *Coordinate Measurement System Committee Conference*, Dearborn, Michigan.
- [13] Brown, J., *V-STARs/S Acceptance Test Results*, [White Paper], Geodetic Services, Inc., Retrieved from <https://www.geodetic.com/wp-content/uploads/2018/08/S-Acceptance-Test-Results-imperial-version.pdf>, Melbourne, Florida .
- [14] *Basics of Photogrammetry*, [White Paper], Geodetic Services, Inc., Retrieved from https://www.geodetic.com/wp-content/uploads/2019/01/Basics_of_Photogrammetry_2017.pdf.
- [15] Peipe, J., 1996, "High Resolution Data Acquisition to Observe Moving Objects," *Int. Arch. Photogramm. Remote Sens.*, **31**, pp. 471–474.
- [16] Wolf, P., and DeWitt, B., 2000, *Elements of Photogrammetry with Applications in GIS*, McGraw-Hill, New York.
- [17] Mikhail, E. M., Bethel, J. S., and McGlone, J. C., 2001, *Introduction to Modern Photogrammetry*, Wiley, New York.
- [18] Solis, E., and Meyn, L., 2016, "Photogrammetric Deflection Measurements for the Tiltrotor Test Rig (TTR) Multi-Component Rotor Balance Calibration," *AHS Technical Meeting on Aeromechanics Design for Vertical Lift*, AHS International, San Francisco, California.
- [19] Creaform, *HandyScan3D: The Truly Portable Metrology-Grade 3D Scanners*, Retrieved from: https://www.creaform3d.com/sites/default/files/assets/brochures/files/handyscan3d_brochure_en_hq_21032017_2.pdf.

- [20] Larue, J.-F., Viala, M., France, C., Brown, D., and Mony, C., 2012, *Dynamic Referencing in 3D Optical Metrology for Higher Accuracy in Shop Floor Conditions*, [White Paper], Creaform, Retrieved from https://www.creaform3d.com/sites/default/files/asets/technological-fundamentals/wp_dynamic-referencing-in-3d-optical-metrology.pdf.
- [21] Russell, C. R., and Sekula, M. K., 2017, "Comprehensive Analysis Modeling of Small-Scale UAS Rotors," *AHS International 73rd Annual Forum & Technology Display*, AHS International, Fort Worth, Texas.
- [22] Allard, P.-H., and Lavoie, J.-A., *Differentiation of 3D Scanners and Their Positioning Method When Applied to Pipeline Integrity*, [White Paper], Creaform, Retrieved from https://www.creaform3d.com/sites/default/files/asets/technological-fundamentals/differentiation_of_3d_scanners_and_their_positioning_method_when_applied_to_pipeline_integrity.pdf, Levis, Quebec City, Canada.
- [23] Lavoie, J.-A., 2015, *THE BENEFITS OF REVERSE ENGINEERING FOR ENSURING PIPELINE INTEGRITY*, [White Paper], Creaform, Retrieved from https://www.creaform3d.com/sites/default/files/asets/technological-fundamentals/benefits_of_reverse_engineering_for_ensuring_pipeline_integrity_en_060502015.pdf.
- [24] Russell, C. R., Theodore, C. R., and Sekula, M. K., 2018, "Incorporating Test Data for Small UAS at the Conceptual Design Level," *AHS International Technical Conference on Aeromechanics Design for Transformative Vertical Flight*, AHS International, San Francisco, California.
- [25] Russell, C., Willink, G., Theodore, C., Jung, J., and Glasner, B., 2018, *Wind Tunnel and Hover Performance Test Results for Multicopter UAS Vehicles*, NASA/TM-2018-219758, Moffett Field, California.